Arylthiazylamides: Syntheses, Structures, and Bonding Properties

Tobias Borrmann,[a] Enno Lork,[b] Rüdiger Mews,*[b] Wolf-Dieter Stohrer,*[a] Paul G. Watson,[b] and Andrey V. Zibarev*[c]

Abstract: Air-sensitive, thermally unstable tris(dimethylamino)sulfonium (TAS) salts (**3**) of the title anions $[ArNSN]^-$ have been prepared from corresponding sulfurdiimides $Ar{-}N{=}S{=}N{-}SiMe_3$ (**2**) by Si−N bond cleavage with $[(Me_2N)_3S]^+[Me_3SiF_2]^-$ (TASF). They are characterized by low-temperature X-ray crystallography as *Z* isomers. Because of the very short terminal S−N distance (144.2 (**3h**) – 147.9 (**3i**) pm) and the relatively long internal S−N distance (158.3 (**3i**) – 160.3 (**3c**) pm) the $[ArNSN]^-$ ions should be regarded as thiazylamides **1b**, rare species containing a S≡N triple bond. A bonding model is developed and the experimental results are compared with those of restricted Hartree – Fock (RHF), density functional theory (DFT), and Møller – Plesset second-order (MP2) calculations.

Keywords: ab initio calculations · arylthiazylamides · multiple bonds · N ligands · S ligands · structure elucidation

Introduction

Previously, it was observed[1–3] that fluoride-ion-induced (CsF in boiling MeCN) intramolecular nucleophilic *ortho*-cyclization of $Ar_F{-}X{-}N{=}S{=}N{-}SiMe_3$ sulfurdiimides makes it possible to obtain, depending on Ar_F and X, the previously unknown and otherwise inaccessible polyfluorinated 2,1,3-benzothiadiazoles (X = -; $Ar_F = 4\text{-}RC_6F_4$),[1] naphtho[1,2-*c*]- and naphtho[2,3-*c*][1,2,5]thiadiazoles (X = -; $Ar_F = 2\text{-}C_{10}F_7$) ,[2] or 1,3,2,4-benzodithiadiazines (X = S; $Ar_F = C_6F_5$).[3] With $Ar_F = 4\text{-}Py_F$ and X = -; S ($4\text{-}Py_F$ = 2,3,5,6-tetrafluoropyrid-4-yl), however, no heterocycles have been prepared, instead polyfluorinated 4-aminopyridine is the major product.[4] The key intermediates in all of these reactions are likely to be the corresponding fluoroarylsulfurdiimide anions, although these species are not observed under the reaction conditions applied. It follows from the available data[1–4] that the reactivity of these intermediate anions $[ArNSN]^-$ toward internal electrophiles (*ortho*-cyclization) depends strongly on the substituents at the $[NSN]^-$ moiety.

Recently,[5] we reported syntheses and structures of $[(Me_2N)_3S]^+$ (TAS^+) salts of two fluoroarylsulfurdiimide anions $[Ar_FNSN]^-$ ($Ar_F = 2\text{-}FC_6H_4$, $2,6\text{-}F_2C_6H_3$). It follows from the X-ray data that, owing to the unexpectedly short terminal S−N bond (for example, 144.2 pm, $Ar_F = 2,6\text{-}F_2C_6H_3$; 145.8 pm, $Ar_F = 2\text{-}FC_6H_4$), these anions should be regarded as thiazylamide (**1b**) rather than sulfurdiimide (**1a**) anions (Scheme 1). Thus, the $[ArNSN]^-$ ions belong to the rare type of compounds featuring S≡N triple bonds and therefore deserve intensive investigation.

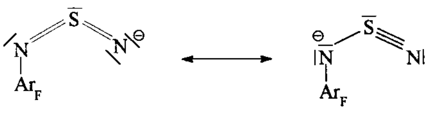

1a **1b**

Scheme 1. Possible representations of $[Ar_FNSN]^-$.

Other structurally characterized $[RNSN]^-$ ions ($R = Me_3C$, Me_3Si) are also best described as thiazylamides.[6] Importantly, this bonding description seems to be more general; a similar change is observed in the $R\bar{N}{=}\bar{S}{=}\underline{\bar{O}}/|N{\equiv}\bar{S}{-}\underline{\bar{O}}|^{\ominus}$ and $R\bar{N}{=}C{=}\bar{N}R/R\underline{\bar{N}}{-}C{\equiv}N|^{\ominus}$ systems.[6]

The present work provides detailed experimental information on the preparation, isolation, and characterization of $[TAS]^+[ArNSN]^-$ salts with various fluoro- and non-fluoroaryl substituents. A bonding model for the $[ArNSN]^-$ system is developed and the influence of the various aryl substituents on the $[NSN]^-$ group is investigated by restricted Hartree – Fock (RHF), density functional theory (DFT), and Møller – Plesset second-order (MP2) methods.

---

[a] Prof. Dr. W.-D. Stohrer, Dr. T. Borrmann
Institute of Organic Chemistry
Bremen University, 28334 Bremen (Germany)
E-mail: stohrer@chemie.uni-bremen.de

[b] Prof. Dr. R. Mews, Dr. E. Lork, Dr. P. G. Watson
Institute for Inorganic and Physical Chemistry
Bremen University, 28334 Bremen (Germany)
E-mail: mews@chemie.uni-bremen.de

[c] Prof. Dr. A. V. Zibarev
Institute of Organic Chemistry
Russian Academy of Sciences
630090 Novosibirsk (Russia)
E-mail: zibarev@nioch.nsc.ru

Results and Discussion

TAS$^+$ salts of arylthiazylamides [ArNSN]$^-$ (3): As previously indicated, the reaction of TASF with *N*-aryl-*N*′-trimethylsilylsulfurdiimides provides an excellent synthetic route to arylthiazylamide salts [TAS]$^+$[ArNSN]$^-$. TASF is available in almost quantitative yield and in high purity from the reaction of SF$_4$ and Me$_2$NSiMe$_3$,[7] *N*-aryl-*N*′-trimethylsilylsulfurdiimides are generally available from the corresponding thionylimides ArNSO and LiN(SiMe$_3$)$_2$, followed by the reaction with Me$_3$SiCl according to Scheme 2.

With TASF in CH$_3$CN solution, cleavage of the Si–N bond readily occurs at − 40 to − 30 °C, independent of the substituents at the aryl ring (Scheme 2). By this route derivatives with donor and acceptor substituents (OCH$_3$, CH$_3$, F, CF$_3$) in *ortho* or *para* positions are readily available. For **3g** (Ar = 4-NO$_2$C$_6$H$_4$) and **3j** (Ar = C$_6$F$_5$), which contain the most electron-withdrawing aryl groups, fast decomposition occurs even at − 40 °C to give unidentified tarry products. This is in contrast to the related carbanion chemistry where acceptor ring substituents stabilize the systems by delocalizing the negative charge.[8]

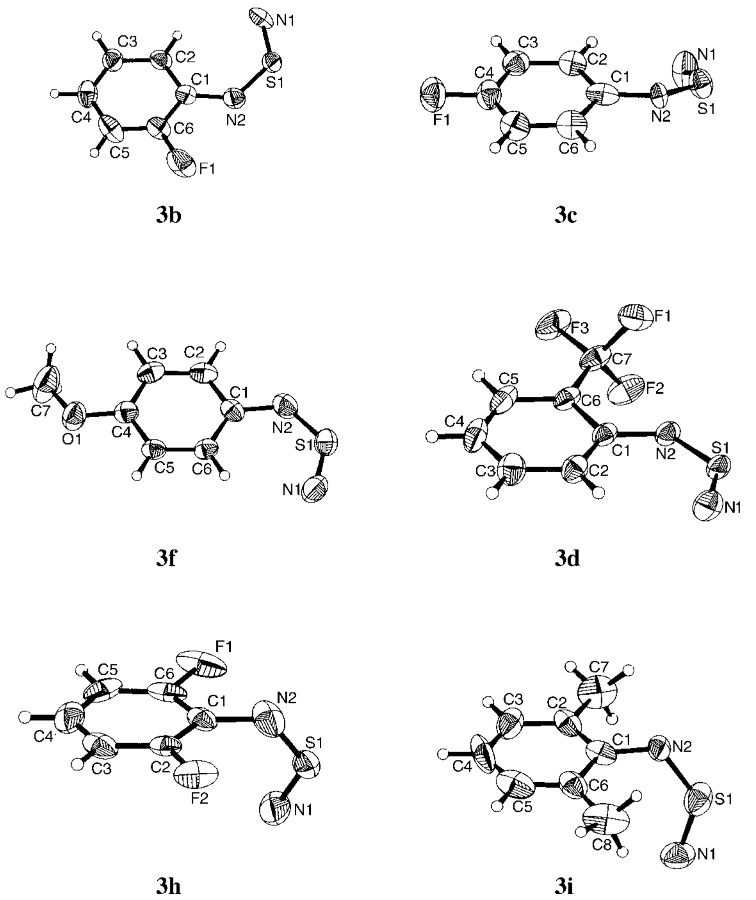

Figure 1. X-ray crystal structures of the anions of [TAS]$^+$[ArNSN]$^-$ (Ar = 4-FC$_6$H$_4$(**3c**), 2-CF$_3$C$_6$H$_4$(**3d**), 4-CH$_3$OC$_6$H$_4$(**3f**), and 2,6-(CH$_3$)$_2$C$_6$H$_3$(**3i**) together with the previously reported[5] **3b** (Ar = 2-FC$_6$H$_4$) and **3h** (Ar = 2,6-F$_2$C$_6$H$_3$) (selected bond lengths [pm] and angles [°] are given in Table 2, τ is the torsion angle between the N-S-N and the ring planes).

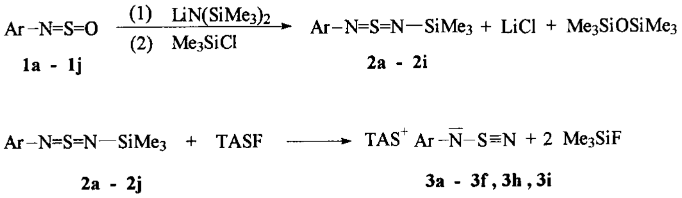

Scheme 2. Syntheses of *N*-aryl-*N*′-trimethylsilylsulfurdiimides and [TAS]$^+$[ArNSN]$^-$. Ar = C$_6$H$_5$ (**a**), 2-FC$_6$H$_4$ (**c**), 2-CF$_3$C$_6$H$_4$ (**e**), 4-CH$_3$OC$_6$H$_4$ (**f**), 4-O$_2$NC$_6$H$_4$ (**g**), 2,6-F$_2$C$_6$H$_3$ (**h**), 2,6-(CH$_3$)$_2$C$_6$H$_3$ (**i**), C$_6$F$_5$ (**j**).

Salts **3a**–**f**,**h**,**i** are orange-yellow solids, stable under vacuum or inert gas atmosphere for at least a few weeks at temperatures below − 20 °C. On warming to room temperature or on contact with air they decompose immediately to give brown tars.

Structure and bonding properties of arylthiazylamides [ArNSN]$^-$ (3): In the case of **3b**–**d**,**f**,**h**,**i** the structures of the salts have been confirmed by low-temperature (− 100 °C) single-crystal X-ray diffraction (Figure 1, Table 1, Table 2. The structures of **3b**,**h** and of the isoelectronic 2,6-F$_2$C$_6$H$_3$NSO have been published previously[5]). Unfortunately, suitable single crystals for X-ray structural analysis of the salts of the parent anion **3a** and its 4-CF$_3$ derivative **3e** could not be obtained.

According to the X-ray data, all of the characterized anions adopt the *Z* configuration in the solid state (Figure 1); the torsion angle between the aryl plane and the N-S-N group ranges from 3.6° (**3f**), 4.4° (**3d**), 6.8° (**3b**), and 26.5° (**3c**) to 70.1° (**3i**) and 75.6–79.0° (**3h**, three independent molecules), depending upon the substituents. The isoelectronic ArNSO compounds[5, 9] (Figure 2, Table 3) also adopt the *Z* configuration in the solid state with the corresponding torsion angle varying from 1.8° to 43.6°. With the analogous fluoroaryl substituent (4-FC$_6$H$_4$NSO and **3c**; 2,6-F$_2$C$_6$H$_3$NSO and **3h**) the torsion angle is larger in the anions, probably reflecting electrostatic repulsion between the F atoms and the [NSN]$^-$ moiety. The terminal S–N$_t$ bond lengths (Table 2), which range from 144.2 (**3h**) to 147.9 pm (**3i**) in the anions of **3**, correspond to the S^{IV}–N triple bond in structurally characterized thiazyl derivatives $R{-}S{\equiv}N$ (142.3 pm, R = (CF$_3$)$_2$N–O;[10] 144.6 pm, R = F;[11] and 145.0 pm, R = Cl[12]). The bridging S–N$_b$ bonds of **3** (Table 2) range from 158.3 (**3i**) to 160.3 pm (**3c**) in length and are between single and double bond lengths (cf. ArNSO: 150.0–151.5 pm)[5, 9] (Figure 2). In

Table 1. Crystal data and structure refinement for **3c,d,f,i**.[a]

	3c	**3d**	**3f**	**3i**
empirical formula	$C_{12}H_{22}FN_5S_2$	$C_{13}H_{22}F_3N_5S_2 \cdot C_2H_3N$	$C_{13}H_{25}N_5OS_2$	$C_{14}H_{27}N_5S_2 \cdot C_2H_3N$
formula weight	319.47	410.53	331.50	370.58
T [K]	173(2)	173(2)	173(2)	173(2)
λ [pm]	71.073	71.073	71.073	71.073
crystal system	monoclinic	monoclinic	monoclinic	monoclinic
space group	$P2_1/c$	$P2_1/c$	$P2_1/n$	$P2_1/c$
unit cell dimensions				
a [pm]	1090.1(3)	786.80(10)	823.40(10)	843.9(2)
b [pm]	1233.7(2)	2721.2(2)	1991.8(2)	1620.5(2)
c [pm]	1219.6(8)	969.40(10)	1098.50(10)	1541.5(3)
β [°]	99.70(3)	101.210(10)	103.360(10)	96.640(10)
volume [nm^3]	1.6167(12)	2.0359(4)	1.7528(3)	2.0939(7)
Z	4	4	4	4
ρ_{calcd} [Mg m^{-3}]	1.312	1.339	1.256	1.176
μ [mm^{-1}]	0.338	0.229	0.310	0.264
$F(000)$	680	864	712	800
crystal size [mm^3]	0.5 × 0.5 × 0.3	0.6 × 0.4 × 0.2	0.8 × 0.5 × 0.15	0.2 × 0.1 × 0.05
θ range [°]	2.51–22.50	2.61–27.50	2.74–22.49	2.51–22.00
index ranges	$-12 \leq h \leq 12$ $-14 \leq k \leq 14$ $-14 \leq l \leq 13$	$-1 \leq h \leq 7$ $-35 \leq k \leq 1$ $-12 \leq l \leq 12$	$-8 \leq h \leq 1$ $-21 \leq k \leq 1$ $-11 \leq l \leq 11$	$-1 \leq h \leq 8$ $-1 \leq k \leq 15$ $-14 \leq l \leq 14$
reflections collected	4432	5400	2980	2707
independent reflections	2110	4096	2190	1953
R_{int}	0.0595	0.0295	0.0327	0.0834
refinement	full-matrix least-squares on F^2	full-matrix least-squares on F^2	full-matrix least-squares on F^2	full-matrix least-squares on F^2
data/restraints/parameters	2107/0/189	4096/0/245	2190/0/209	1953/0/229
goodness of fit on F^2	1.033	1.022	1.003	0.574
final R indices [$I > 2\sigma(I)$]				
$R1$	0.0636	0.0439	0.0505	0.0431
$wR2$	0.1582	0.0951	0.1168	0.0679
R indices (all data)				
$R1$	0.0983	0.0723	0.0835	0.1461
$wR2$	0.1799	0.1070	0.1334	0.0868
extinction coefficient	–	0.0033(6)	0.0046(12)	0.0014(4)
largest diff. peak/hole [e nm^{-3}]	494/ – 301	307/ – 301	246/ – 250	167/ – 181

[a] See also ref. [15].

Table 2. Selected bond lengths [pm] and angles [°] in arylthiazylamides.[a]

Aryl	$C_{Ar}N$	N_bS	SN_t	N_bSN_t	$C_{Ar}N_bS$	τ	Ref
3d	139.2(2)	159.3(2)	147.5(2)	125.9(1)	126.8(2)	4.4(2)	
3h[b]	140.7	158.9	144.2	122.3	119.0	77.7	5
3b	139.0(6)	159.9(4)	145.8(4)	124.8(2)	126.5(3)	6.8(5)	5
3c	138.8(7)	160.3(5)	146.9(5)	124.5(3)	126.0(4)	26.5(3)	
3i	138.5(8)	158.3(5)	147.9(5)	124.7(3)	122.0(4)	70.1(3)	
3f	141.0(5)	158.6(4)	147.3(4)	125.5(2)	127.1(3)	3.6(4)	

[a] The anions are arranged in decreasing order of the calculated acceptor strength of the aryl group (see Figure 4a–c and Tables 4 and 5).[b] Average data for three crystallographically independent molecules.

thiazyl derivatives RSN the bond angle at S is 117–119°, in the anions of **3** the N-S-N angle is widened to 122.7 (**3h**)–125.9° (**3d**), and in ArNSO the N-S-O angle is 120–121°.

The available data (see references [5, 9]; Figure 1 and 2; Table 2) also demonstrate that the geometry of the NSO group in ArNSO compounds (only a few examples of which were structurally characterized[9] before our work) is practically independent of the conformation (planar or twisted) as well as of the nature of the carbocyclic substituents. This is in contrast to the geometry of the $[NSN]^-$ moiety in $[ArNSN]^-$ ions.

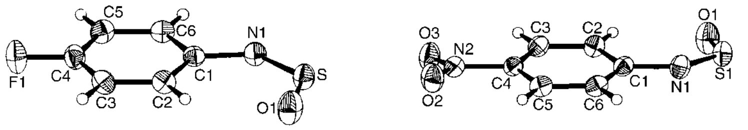

4 **5**

Figure 2. X-ray crystal structures of 4-FC_6H_4NSO (**4**) and 4-O_2N-C_6H_4NSO (**5**) with selected bond lengths [pm] and angles [°]: **4**: C1–N1 140.7(2), N1–S1 151.50(15), S1–O1 145.6(1); C1-N15-S1 132.5(1), N1-S1-O1 119.8(1); τ 1.8(1). **5**: C1–N1 141.1(1), N1–S1 151.5(1) S1–O1 145.1(1); C1-N1-S1 131.9(1), N1-S1-O1 120.3(1); τ 7.8 (1).

Bonding model for arylthiazylamides $[ArNSN]^-$ (3): The detailed bonding description of $[RNSN]^-$ ions ($R = Me_3C$, Me_3Si) was reported previously.[6] Theoretical considerations of the present work focus on the description of the π system of the $[NSN]^-$ fragment including the effects of the π-donor/acceptor properties of the aryl group upon it, and the effect of twisting around the C_{Ar}–N_b bond caused by steric and/or electrostatic interactions.

Calculations for the title anions at the RHF/6-311+G*, B3LYP/6-311+G*, and MP2/6-311+G* levels of theory were carried out to study these effects (Tables 4–6, respective-

Table 3. Crystal data and structure refinement for **4** and **5**.[a]

	4	**5**
empirical formula	C_6H_4FNOS	$C_6H_4N_2O_3S$
formula weight	157.16	184.17
T [K]	173(2)	173(2)
λ [pm]	71.073	71.073
crystal system	monoclinic	monoclinic
space group	$P2_1/n$	$P2_1/c$
unit cell dimensions		
a [pm]	381.50(10)	373.20(10)
b [pm]	2017.9(3)	988.70(10)
c [pm]	853.1(2)	2001.7 (4)
β [°]	97.73(3)	90.81
volume [nm^3]	0.6508(2)	0.7385(3)
Z	4	4
ρ_{calcd} [Mg m^{-3}]	1.604	1.656
μ [mm^{-1}]	0.435	0.401
F(000)	320	376
crystal size [mm^3]	$0.70 \times 0.40 \times 0.20$	$0.6 \times 0.5 \times 0.4$
θ range [°]	2.61–27.48	2.90–27.52
index ranges	$-1 \le h \le 4$ $-26 \le k \le 26$ $-11 \le l \le 11$	$-1 \le h \le 4$ $-12 \le k \le 12$ $-23 \le l \le 26$
reflections collected	3990	4475
independent reflections	1347	1666
R_{int}	0.0312	0.0412
refinement	full-matrix least-squares on F^2	full-matrix least-squares on F^2
data/restraints/parameters	1347/0/93	1666/0/111
goodness of fit on F^2	1.046	1.076
final R indices [$I > 2\sigma(I)$]		
$R1$	0.0323	0.0317
$wR2$	0.0815	0.0839
R indices (all data)		
R1	0.0395	0.0389
wR2	0.0860	0.0876
extinction coefficient	0.019(3)	0.0079(16)
largest diff. peak/hole [e nm^{-3}]	236/–319	252/–241

[a] See also ref. [15].

Table 4. Bond lengths and torsion angles in selected arylthiazylamides calculated at the RHF/6–311+G* level of theory.

Aryl	r_{CO} [pm] (ArO$^-$)	r_{CNb} [pm] (ArNSN$^-$)	r_{NbS}[pm] (ArNSN$^-$)	r_{SNt} [pm] (ArNSN$^-$)	τ_{CCNbS} [°] (ArNSN$^-$)	NIMAG[a] (ArNSN$^-$)
p-NO$_2$ (**3g**)[b]	122.49	133.75	161.14	146.88	0.0	0
C_6F_5 (**3j**)[b]	123.48	136.01	160.38	146.19	56.0	0
o-CF$_3$ (**3d**)	123.55	134.91	159.76	146.89	0.0	0
2,6-F$_2$ (**3h**)	123.97	136.73	159.60	146.28	57.7	0
o-F (**3b**)	124.26	135.87	159.13	146.92	0.0	0
o-F, twisted	124.26	137.35	158.93	146.44	60.0 fix	–
Ph (**3a**)[c]	124.66	136.52	159.04	146.94	0.0	0
p-F (**3c**)	125.01	136.90	158.85	146.92	0.0	0
p-F, twisted	125.01	138.28	158.83	146.47	60.0 fix	–
2,6-Me$_2$ (**3i**)	125.22	138.34	158.22	146.46	62.4	0
p-OMe (**3f**)	125.32	137.28	158.55	146.92	0.0	0

[a] Number of imaginary frequencies: 0 = confirms a minimum, – = not calculated. [b] Not isolated. [c] Not structurally characterized.

Table 5. Bond lengths and torsion angles in selected arylthiazylamides calculated at the B3LYP/6–311+G* level of theory.

Aryl	r_{CO} [pm] (ArO$^-$)	r_{CNb} [pm] (ArNSN$^-$)	r_{NbS}[pm] (ArNSN$^-$)	r_{SNt} [pm] (ArNSN$^-$)	τ_{CCNbS} [°] (ArNSN$^-$)	NIMAG[a] (ArNSN$^-$)
p-NO$_2$ (**3g**)[b]	125.33	135.22	166.70	150.36	0.0	0
C_6F_5 (**3j**)[b]	125.60	136.27	166.32	149.54	53.0	0
o-CF$_3$ (**3d**)	125.75	135.97	165.24	150.60	0.0	0
2,6-F$_2$ (**3h**)	125.97	136.67	165.61	149.76	53.0	0
o-F (**3b**)	126.44	136.67	164.74	150.72	0.0	0
o-F, twisted	126.44	137.39	165.01	150.14	53.0 fix	–
Ph (**3a**)[c]	126.96	137.38	164.59	150.79	0.0	0
p-F (**3c**)	127.04	137.51	164.51	150.78	0.0	0
p-F, twisted	127.04	138.22	164.89	150.26	53.0 fix	–
2,6-Me$_2$ (**3i**)	127.50	138.18	164.08	150.28	54.1	0
p-OMe (**3f**)	127.29	137.75	164.31	150.86	0.0	0

[a] Number of imaginary frequencies: 0 = confirms a minimum, – = not calculated. [b] Not isolated. [c] Not structurally characterized.

Table 6. Bond lengths and torsion angles in selected arylthiazylamides calculated at the MP2/6–311+G* level of theory.

Aryl	r_{CO} [pm] (ArO$^-$)	r_{CNb} [pm] (ArNSN$^-$)	r_{NbS}[pm] (ArNSN$^-$)	r_{SNt} [pm] (ArNSN$^-$)	τ_{CCNbS} [°] (ArNSN$^-$)	NIMAG[a] (ArNSN$^-$)
p-NO$_2$ (**3g**)[b]	126.14	138.06	163.27	149.65	0.0	-
C_6F_5 (**3j**)[b]	126.31	138.15	163.66	149.07	58.8	-
o-CF$_3$ (**3d**)	126.53	138.32	162.47	150.09	0.0	-
2,6-F$_2$ (**3h**)	126.56	138.32	163.02	149.37	58.0	-
o-F (**3b**)	127.01	138.64	162.19	150.29	0.0	-
o-F, twisted	127.01	139.03	162.58	149.81	58.0 fix	-
Ph (**3a**)[c]	127.53	139.39	161.96	150.42	0.0	-
p-F (**3c**)	127.62	139.40	161.97	150.46	0.0	-
p-F, twisted	127.62	139.78	162.40	149.93	58.0 fix	-
2,6-Me$_2$ (**3i**)	128.16	139.64	162.03	150.19	57.8	-
p-OMe (**3f**)	127.80	139.48	161.89	150.60	0.0	-

[a] Number of imaginary frequencies: 0 = confirms a minimum, – = not calculated. [b] Not isolated. [c] Not structurally characterized.

ly). Additional calculations for the analogous phenolates (where no twisting is possible) were performed to observe the influence of only the donor/acceptor strength of the aryl group on the observed bond lengths. This made it possible to interpret the influence of each effect independently of the other. The C_{Ar}–O bond lengths thus calculated serve as an indicator for the donor/acceptor strength of the aryl groups (Tables 4–6). The analyzed bond length dependencies are based upon RHF calculations (Table 4) and are confirmed by B3LYP (Table 5) and MP2 (Table 6) calculations.

The correlation of the calculated phenolate C_{Ar}–O and C_{Ar}–N_b bond lengths of the thiazylamides is, as expected, very good for the planar anions. The dependence of the bond length on the acceptor strength is evident; the stronger the acceptor, the shorter is the C_{Ar}–O or the C_{Ar}–N_b bond length respectively (Figure 3a).

The influence of the twisting around the C_{Ar}–N_b bond is also evident and for three selected anions **3i**, **3h**, and **3j** it is virtually the same; the bond lengths increase by around 1.2 pm.

The correlation between C_{Ar}–O bond lengths and N_b–S or S–N_t bond lengths is less evident. The N_b–S bond becomes longer (Figure 3b) with increasing acceptor strength and remains virtually independent of twisting of the planes with respect to each other. The decrease of the S–N_t bond length (Figure 3c) with increasing acceptor strength is very small, however, twisting of the aryl plane by approximately 60° leads to a considerable shortening of this bond.

The dependence of the bond lengths on the acceptor strength is most easily explained by a very simple qualitative description of the π interaction between the HOMO of the $[NSN]^{2-}$ fragment and an empty p orbital of a substituent. This interaction transforms the completely nonbonding

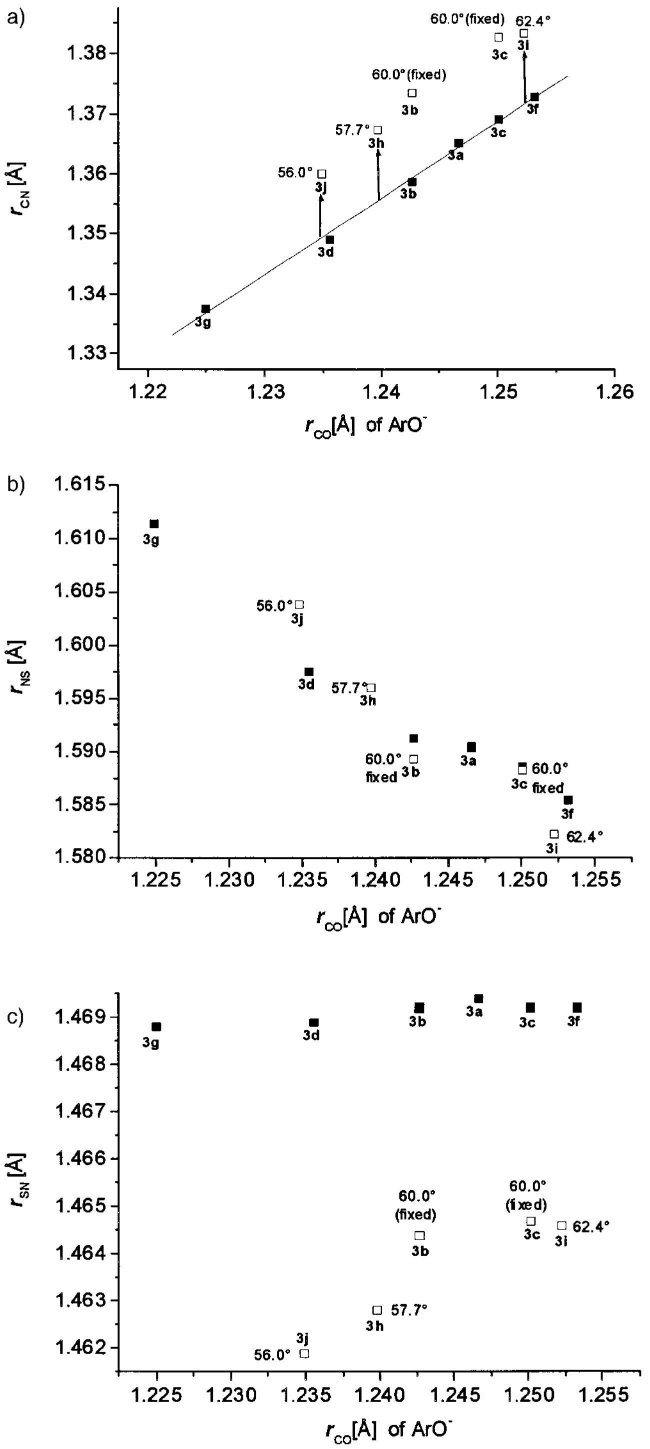

Figure 3. RHF/6-311+G* calculated bond lengths r in [ArNSN]$^-$: a) C–N; b) N_b–S; c) S–N_t. The bond lengths are plotted against that of C–O in ArO$^-$, which serves as an indicator of the acceptor strength. The planar compounds are marked by ■. The twisted compounds are marked by □; those with fixed torsion angles are labeled, the others have relaxed torsion angles.

Table 7. Dependence of RHF-calculated bond lengths on aryl's acceptor strength and twisting of aryl and N-S-N planes.

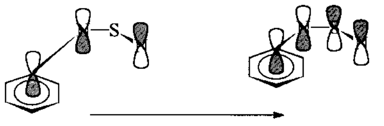 increasing acceptor strength			
increases $\pi_{NSN} \rightarrow \pi_{Ar}$, thus increasing:	bonding character CN_b	antibonding character N_bS	bonding character SN_t
	r_{CNb} shorter	r_{NbS} longer	r_{SNt} shorter
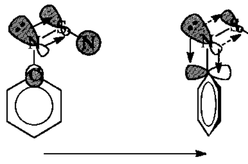 increasing torsion angle			
decreases $\pi_{NSN} \rightarrow \pi_{Ar}$, thus decreasing:	**bonding character CN_b**	antibonding character N_bS	bonding character SN_t
	r_{CNb} longer	r_{NbS} shorter	r_{SNt} longer
increases $n_N \rightarrow \pi_{Ar}$, thus increasing:	bonding character CN_b		
and decreasing:		bonding character N_bS	**antibonding character SN_t**
	r_{CNb} shorter	r_{NbS} longer	**r_{SNt} shorter**
RHF-calculated bond length	longer	no change	shorter

allylic-like HOMO of the [NSN]$^{2-}$ fragment into a butadiene type HOMO, as shown in Table 7. Thus the completely nonbonding character of the HOMO in the [NSN]$^{2-}$ changes into an orbital that is bonding in the Ar–N_b and S–N_t regions and antibonding in the N_b–S region, respectively, therefore changing these bonds in the calculated manner. This change in bond lengths becomes more pronounced as the above-described orbital interaction becomes stronger, that is, as the acceptor strength increases.

The lengthening, and thus weakening, of the N_b–S bond with the increase of the acceptor strength of the Ar group explains the decreased stability of the title anions with the most electron-withdrawing aryl groups (4-$O_2NC_6H_4$, C_6F_5), as discussed previously. We assume that this instability is associated with a cleavage of the N_b–S bond. Such cleavage should lead to $ArNH_2$ as the final product. Indeed, in the case of Ar = 4-Py_F, which is also a strong acceptor substituent (see Introduction), the corresponding 4-Py_FNH_2 was isolated from the reaction mixture in high yield.[4]

In the qualitative description of the dependence of the bond lengths on the twisting around the C_{Ar}–N_b axis one must not only consider the π,π interaction described above but also the n,π interaction with the lone pair of electrons on the bridging nitrogen atom (Table 7). The lone pair of electrons of the nitrogen atom in the planar [RNSN]$^-$ ions interacts only with the σ* orbital of the terminal S–N_t bond with bonding character in the N_b–S region and antibonding in the region of the S–N_t bond.[6] If the aryl group is twisted with respect to the N-S-N plane, the nitrogen lone pair can donate electron density into the π system of the aryl group. This weakens the interaction with the σ* orbital of the terminal S–N_t bond with the result that the bonding is strengthened in the C_{Ar}–N_b and S–N_t regions and the bonding is weakened in the N_b–S region.

Consequently, there are two opposing effects on twisting around the C_{Ar}–N_b bond (Table 7). The π,π interaction results in a weakening of the C_{Ar}–N_b and S–N_t bonds and a strengthening of the N_b–S bond. The n,π interaction on the other hand leads to a strengthening of the C_{Ar}–N_b and S–N_t bonds and a weakening of the N_b–S bond. Observations show a longer C_{Ar}–N_b bond, a virtually unchanged N_b–S bond, and a shorter S–N_t bond. Thus the π,π interaction dominates in the C_{Ar}–N bond region and the n,π interaction dominates in the S–N_t bond region, and in the region of the N_b–S bond they cancel each other out.

Thus, the bonding model for alkylthiazylamides[6] is now extended to arylthiazylamides, and the dependence of N–S and N–C bond lengths on acceptor strength and twisting can be explained with the extended model. However, the agreement of the calculated geometries with those from X-ray structural analysis is not particularly good. Partial optimizations of **3a** at the RHF/6-311+G* level show only small energy differences (max. 1.6 kJ mol^{-1}) on changing the bond lengths from equilibrium to the extremes of **3g** and **3f**, respectively (Table 8). We have previously[6] shown that energy differences between *E,Z* conformers (up to 17 kJ mol^{-1}) are easily compensated by anion–cation interactions. Altogether, these data indicate that a comparison of theoretical (free molecules) and experimental (solid state) geometries of $[ArNSN]^-$ ions is complicated by solid-state effects.

Table 8. RHF/6–311+G* calculated energy differences for optimized and model conformations of $PhNSN^-$ (**3a**).

3a	Bond lengths optimized [pm]	fixed [pm]	Energy ΔE [kJ mol^{-1}]
$C_{Ar}N_b$	136.52	133.75 (**3g**)	1.6
N_bS	159.04	161.14 (**3g**)	0.7
$C_{Ar}N_b$	136.52	137.28 (**3f**)	0.1
N_bS	159.04	158.55 (**3f**)	< 0.1

Conclusion

The arylthiazylamides prepared and structurally characterized in this work represent a new class of sulfur–nitrogen anions. Importantly, they are thiazyl compounds, a rare type of compounds containing a S≡N triple bond, rather than N=S=N derivatives. A qualitative bonding model is proposed, which accounts for the influence of the acceptor strength and/or twisting of the aryl groups on the bond lengths. The quantitatively calculated effects, however, are rather small, so that they are easily overcome by intermolecular interactions in the experimentally determined structures in the solid state.

Experimental Section

General: The ^1H and ^{19}F NMR spectra were recorded on a Bruker DPX-200 spectrometer, for $CDCl_3$ solutions at frequencies of 200.13 and 188.28 MHz, respectively. Chemical shifts are given with respect to TMS and $CFCl_3$. The high-resolution mass spectra (EI, 70 eV) were measured with a Finnigan MAT MS 8200 mass spectrometer. TASF was prepared by established methods.[7] Syntheses were performed under an argon atmosphere, in dry solvents with stirring. The reagents were added dropwise and the solvents were distilled off under reduced pressure. Compounds **2a**, **2g**, **2i**, and **2j**,[18] were prepared as previously reported. Table 9 lists the physical and analytical data for the compounds synthesized.

Table 9. Characterization of *N*-aryl-*N*′-silylsulfurdiimides.

Compound	Yield [%]	b.p. [°C/mm]	NMR, δ [ppm] ^1H	^{19}F	Molecular formula [MS: M^+ [*m/z*], measured(calculated)]
2b	85	63–64/0.01	7.73 (1H), 7.16–7.06 (3H), 0.17 (9H)	– 118.5	$C_9H_{13}FN_2SSi$: 228.0549 (228.0553)
2c	90	80–81/0.01	7.87 (2H), 7.02 (2H), 0.31 (9H)	– 112.7	$C_9H_{13}FN_2SSi$: 228.0552 (228.0553)
2d	80	74–75/0.01	7.77 (1H), 7.73 (1H), 7.57 (1H), 7.30 (1H), 0.25 (9H)	– 62.0	$C_{10}H_{13}F_3N_2SSi$: 278.0525 (278.0521)
2e	70	67–68/0.01	7.78 (2H) 7.70 (2H), 0.37 (9H)	– 62.8	$C_{10}H_{13}F_3N_2SSi$: 278.0523 (278.0521)
2f	70	83–84/0.01	8.04 (2H), 6.29 (2H), 3.84 (2H), 0.37 (9H)	–	$C_{10}H_{16}N_2OSSi$: 240.0759 (240.0753)
2h	80	64–65/0.01	7.05–6.84 (3H), 0.15 (9H)	– 116.9	$C_9H_{12}F_2N_2SSi$: 246.0463 (246.0459)

Crystallographic analysis: The single-crystal X-ray structure determinations (Tables 1 and 3) were carried out on a Siemens P4 diffractometer using $Mo_{K\alpha}$ (0.71073 Å) radiation with a graphite monochromator. Refinement based on F^2; $R1 = \Sigma||F_o| - |F_c||$; $wR2 = \{\Sigma[w(F_o^2 - F_c^2)^2/\Sigma[w(F_o^2)^2]\}^{1/2}$. Programs used: SHELX-97[13] and DIAMOND.[14] The structures were solved by direct methods (SHELXS).[13] Subsequent least-squares refinement (SHELXL 97–2)[13] located the positions of the remaining atoms in the electron density maps. All non-hydrogen atoms were refined anisotropically.[15] The crystals were mounted using KEL-F oil on a thin glass fiber. Single crystals of $4\text{-}FC_6H_4NSO$ (**4**)[16] and $4\text{-}O_2NC_6H_4NSO$ (**5**)[16] were prepared by recrystallization from hexane, for **4** at – 40 °C.

Computational methods: All quantum-chemical calculations were performed with the Gaussian 98 program.[17] The fully optimized structures were confirmed with frequency analyses only for RHF and B3LYP calculations.

1-Aryl-3-trimethylsilyl sulfurdiimides (2b–f, h): A solution of the appropriate ArNSO[16] (60 mmol) in hexane (25 mL) was added to a suspension of $LiN(SiMe_3)_2$ (10.0 g, 60 mmol) in hexane (50 mL) at – 30°C. The temperature was raised to 20 °C over 2 h, then a solution of Me_3SiCl (6.6 g, 60 mmol) in hexane (10 mL) was added. The precipitate was filtered off, the solvent distilled off, and the residue distilled under vacuum. Compounds **2b–f** and **2h** were obtained as orange oils.

Tris(dimethylamino)sulfonium arylthiazylamides (3a–f,h,i): TASF (1.37 g, 5 mmol) was placed into one side of a two-armed λ-shaped glass vessel fitted with a Teflon valve, the appropriate $Ar{-}N{=}S{=}N{-}SiMe_3$ (**2a–f,h,i**) (5 mmol) was placed into the other side with a syringe under dry argon. Through a vacuum line CH_3CN (20 mL) was distilled onto the TASF at – 196 °C, this solution was mixed with **2** at – 40 °C. After 2 h at this temperature, Et_2O (30 mL) was condensed onto the reaction mixture at – 196 °C and the λ-tube was placed into a cryostat at – 40 °C for crystal growth. Salts **3a–f,h,i** were obtained as orange-yellow crystalline solids after removal of the solvents with a syringe under dry argon at – 40 °C. Because of their thermal instability the salts were characterized only by low-temperature X-ray crystallography.

Acknowledgements

The authors are grateful to Peter Brackmann for technical assistance, and to the Deutsche Forschungsgemeinschaft (Germany) and the Russian Foundation for Basic Research (Russia) for joint financial support of this work (DFG: 436 RUS 113/486/0; RFBR: 98–03–04107). A.Z. is also grateful to the Royal Society of Chemistry (UK) for a RSC Journals Grant for International Authors.

---

[1] A. V. Zibarev, A. O. Miller, *J. Fluor. Chem.* **1990**, *50*, 359.

[2] I. Yu. Bagryanskaya, Yu. V. Gatilov, A. O. Miller, M. M. Shakirov, A. V. Zibarev, *Heteroatom Chem.* **1994**, *5*, 561.

[3] A. V. Zibarev, Yu. V. Gatilov, A. O. Miller, *Polyhedron* **1992**, *11*, 1137.

[4] I. Yu. Bagryanskaya, Yu. V. Gatilov, A. Yu. Makarov, A. M. Maksimov, A. O. Miller, M. M. Shakirov, A. V. Zibarev, *Heteroatom Chem.* **1999**, *10*, 113.

[5] A. V. Zibarev, E. Lork, R. Mews, *Chem. Commun.* **1998**, 991.

[6] T. Borrmann, A. V. Zibarev, E. Lork, G. Knitter, S.-J. Chen, P. G. Watson, E. Cutin, M. M. Shakirov, W.-D. Stohrer, R. Mews, *Inorg. Chem.* **2000**, *39*, 3999.

[7] W. J. Middleton, *Org. Synth.* **1985**, *84*, 221.

[8] a) D. J. Cram, *Fundamentals of Carbanion Chemistry*, Academic Press, New York, **1965**; b) *Comprehensive Carbanion Chemistry* (Eds.: E. Buncel, T. Durst), Elsevier, Amsterdam, **1980**; c) R. B. Bates, C. A. Ogle, *Carbanion Chemistry*, Springer, Berlin, **1983**; d) *Stable Carbanion Chemistry* (Eds.:G. K. S. Prakash, P. von R. Schleyer), Wiley, New York, **1997**.

[9] a) R. N. Butler, J. P. Duffy, P. McArdle, D. Cunningham, G. A. O'Halloran, *J. Chem. Soc. Chem. Commun.* **1989**, 1210; b) H. W. Roesky, K. L. Weber, M. Noltemeyer, G. M. Sheldrick, *Z. Naturforsch. B* **1984**, *39b*, 163; c) F. Iwasaki, *Acta Crystallogr. Sect. B* **1980**, *36*, 1700.

[10] G. Hartmann, R. Mews, G. M. Sheldrick, R. Anderskewitz, M. Niemeyer, H. J. Emeleus, H. Oberhammer, *J. Fluor. Chem.* **1986**, *34*, 46.

[11] R. L. Cook, W. H. Kirchhoff, *J. Chem. Phys.* **1967**, *47*, 4521.

[12] a) T. Beppo, E. Hirota, Y. Morino, *J. Mol. Spectrosc.* **1970**, *36*, 386; b) W. C. Emken, K. Hedberg, *J. Chem. Phys.* **1973**, *58*, 2195.

[13] G. M. Sheldrick, SHELX-97, University of Göttingen, Göttingen, Germany, 1997.

[14] DIAMOND-Visual Crystal Structure Information System, Crystal Impact, Bonn, Germany.

[15] Crystallographic data (excluding structure factors) for the structures reported in this paper have been deposited with the Cambridge Crystallographic Data Centre as supplementary publication nos. CCDC-153116 (**3c**), CCDC-153113 (**3d**), CCDC-153114 (**3f**), CCDC-153110 (**3i**), CCDC-153115 (**4**), and CCDC-153111 (**5**). Copies of the data can be obtained free of charge on application to CCDC, 12 Union Road, Cambridge CB2 1EZ, UK, (fax: (+44)1223-336033; e-mail: deposit@ccdc.cam.ac.uk).

[16] *Gmelin Handbook of Inorganic Chemistry, Sulfur-Nitrogen Compounds, Part 6*, Springer, Berlin, **1990**, pp. 113–171.

[17] Gaussian 98 (Revision A.7), M. J. Frisch, G. W. Trucks, H. B. Schlegel, G. E. Scuseria, M. A. Robb, J. R. Cheeseman, V. G. Zakrzewski, J. A. Montgomery, R. E. Stratman, J. C. Burant, S. Dapprich, J. M. Millam, A. D. Daniels, K. N. Kudin, M. C. Strain, O. Farkas, J. Tomasi, V. Barone, M. Cossi, R. Cammi, B. Menucci, C. Pomelli, C. Adamo, S. Clifford, J. Ochterski, G. A. Peterson, P. Y. Ayala, Q. Cui, K. Morokuma, D. K. Malick, A. D. Rabuck, K. Raghavachari, J. B. Foresman, J. Cioslovski, J. V. Ortiz, A. G. Boboul, B. B. Stefanov, G. Liu, A. Liashenko, P. Piskorz, I. Komaromi, R. Gomperts, R. L. Martin, D. J. Fox, T. Keith, M. A. Al-Laham, C. Y. Peng, A. Nanayakkara, C. Gonzales, M. Challacombe, P. M. W. Gill, B. Jonson, W. Chen, M. W. Wong, J. L. Andres, C. Gonzales, M. Head-Gordon, E. S. Replogle, J. A. Pople, Gaussian, Inc. Pittsburgh PA, **1998**.

[18] A. V. Zibarev, A. O. Miller, Yu. V. Gatilov, G. G. Furin, *Heteroatom Chem.* **1990**, 1, 443.

Received: December 18, 2000 [F2945]